# Thermally Charged Capacitors

*In Review - Phys. Rev. Lett. (2003)*

D.P. Sheehan*, A.R. Putnam‡ and J.H. Wright†
* Department of Physics
† Department of Mathematics and Computer Science
University of San Diego, San Diego, CA 92110
‡ Department of Computer Engineering
University of Washington, Seattle, WA
619-260-4095, FAX: 619-260-6874
dsheehan@sandiego.edu

September 29, 2003

**Abstract**

A new class of microscopic solid-state capacitors is identified that charges solely by thermal processes and which can, in principle, remain poised for discharge indefinitely. 2-D numerical simulations verify principal results of a 1-D analytic model. Device energy and power densities appear sufficient to power select micro- and nano-scale devices.

Key Words: nanotechnology, MEMS, NEMS, thermodynamics, capacitors
PACS: 84.32.Tt, 85.30.-z

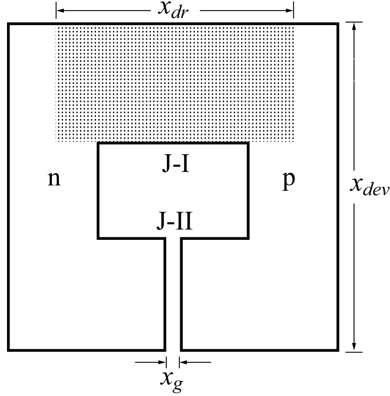


Figure 1: Standard device with Junctions I and II and physical variables indicated. The J-I depletion region is shaded.

Capacitors are reservoirs for electrostatic energy, storing charge at an electrostatic potential. While capacitance is a geometric/compositional quantity intrinsic to the capacitor itself, charge and potential are normally set by an extrinsic work source. In this Letter, we report on a capacitor whose electrostatic energy derives not from extrinsic work, but instead from intrinsic thermal processes. This will be called a *thermal capacitor*. Whereas standard capacitors dissipate their electrostatic energy through internal parasitic resistance ($R_i$) on a timescale $\tau \sim R_i C$, thermal capacitors can remain energized indefinitely. As such, they can be reservoirs of ready energy or local sources for static electric fields.

Consider a p-n device (Fig. 1, consisting of two mirror-symmetric horseshoe-shaped pieces of n- and p-semiconductor facing one another. At Junction I (J-I), the n- and p-regions are physically connected forming a standard p-n junction, while at Junction II (J-II) there is a vacuum gap whose width ($x_g$) we take small compared to the scale lengths of either the depletion region ($x_{dr}$) or the overall device ($x_{dev}$); that is, $x_g \ll x_{dr} \sim x_{dev}$. Let the n- and p-regions be uniformly doped; the p-n junction is taken to be a step junction (graded junctions render similar results); diffusion of donor (D) and acceptor (A) impurities is negligible; the depletion approximation holds; impurities are completely ionized; the semiconductor dielectric is linear. For a silicon device as in Fig. 1, representative physical parameters meeting these conditions are: $N_A = N_D = 10^{21}$ m$^{-3}$, $x_{dev} = 10^{-6}$ m, and $x_g = 3 \times 10^{-8}$m. The p-n device with these parameters will be called the *standard device*.

When individual n- and p- materials are joined, charge carriers cross-diffuse between the n- and p-regions forming the depletion region; widths range from $10\mu m$ for lightly-doped semiconductor to $0.01\mu m$ for heavily-doped ones. Space charge separation gives rise to a built-in potential (typical values, $V_{bi} \sim 1$V) and an internal electric field which arrests further charge diffusion. Standard

one-dimensional formulae predict $x_{dr} = 1.2 \times 10^{-6}$ m and $V_{bi} \simeq 0.6$ V for the *standard device*:

$$V_{bi} = \frac{kT}{q} ln(\frac{N_A N_D}{n_i^2}); \qquad x_{dr} = \left[\frac{2\kappa\epsilon_o V_{bi}}{q}\frac{(N_A+N_D)}{N_A N_D}\right]^{\frac{1}{2}} \tag{1}$$

Here $kT$ is the thermal energy; $q$ is an electronic charge; $n_i$ is the intrinsic carrier concentration of silicon ($n_i \simeq 1.2 \times 10^{16}$ m$^{-3}$ at 300K); $\epsilon_o$ is the permitivity of free space; and $\kappa = 11.8$ is the dielectric constant for silicon.

Physical properties vary continuously with position across the J-I region (Fig. 1), but across open-gap J-II there are marked discontinuities in energy, voltage and charge because of charge carriers' inability to jump the vacuum gap ($x_g$), thus disallowing charge diffusion which would otherwise spatially smooth physical properties. Because the J-II gap is narrow and since the potential changes $V_{bi}$ across it, there can be large gap electric fields ($E_{J-II} \sim \frac{V_{bi}}{x_g}$), more than an order of magnitude greater than in the J-I depletion region.

That an electric field exists in the J-II gap at equilibrium can be established either via Kirchhoff's loop rule or via Faraday's law. Consider a vectorial loop threading the J-I depletion region, the bulk of *standard device*, and the J-II gap. Since the electric field in the J-I depletion region is unidirectional, there must be a second electric field somewhere else along the loop to satisfy Faraday's law ($\oint \mathbf{E} \cdot d\mathbf{l} = 0$). An electric field elsewhere in the semiconductor bulk (other than in the depletion region), however, would generate a current, which contradicts the assumption of equilibrium. Therefore, by exclusion, the other electric field must exist in the J-II gap. Kirchhoff's loop rule establishes the same result.

Treating the gap one-dimensionally, the J-II electric field is uniform, with $|\mathbf{E_{J-II}}| \simeq \frac{V_{bi}}{x_g}$, while in the J-I bulk material it has a triangular profile, with average magnitude $|\mathbf{E_{J-I}}| \sim \frac{V_{bi}}{x_{dr}}$. The ratio of the electric field strength in the J-II gap to that in the middle of the J-I depletion region scales as $\frac{\mathbf{E_{J-II}}}{\mathbf{E_{J-I}}} \sim \frac{x_{dr}}{x_g} \gg 1$. For the *standard device*, the average value field strengths are $|\mathbf{E_I}| \sim \frac{0.6V}{1.2\times10^{-6}m} \simeq 5 \times 10^5$ V/m and $|\mathbf{E_{II}}| \sim \frac{0.6V}{3\times10^{-8}m} \sim 2 \times 10^7$ V/m, rendering $\frac{\mathbf{E_{J-II}}}{\mathbf{E_{J-I}}} \sim 40$. Since electrostatic energy density scales as $\rho_e \sim E^2$, one has $\rho_{e,J-II} \gg \rho_{e,J-I}$.

Theoretical limits to the energy released from J-II in its transition from an open- to a closed-gap configuration can be estimated from the total electrostatic energy $\mathcal{E}_{es}$ inherent to the J-II junction. Let $\Delta\mathcal{E}_{es}(J-II)$ be the difference in electrostatic energy in J-II between its closed- and opened-gap equilibrium states. Within 1-D model constraints, this is:

$$\Delta\mathcal{E}_{es}(J-II) \simeq \frac{\epsilon_o}{2}[\frac{x_{dr}kT}{q} ln(\frac{N_A N_D}{n_i^2})]^2 \cdot [\frac{1}{x_g} - \frac{1}{3}\frac{\kappa}{x_{dr}}], \tag{2}$$

Eliminating $V_{bi}$ and $x_{dr}$ with (1) and setting $N_A = N_D \equiv N$, this can be recast as:

$$\Delta\mathcal{E}_{es}(J-II) \simeq \frac{16\kappa\epsilon_o^2}{qN}\left\{\frac{kT}{q} ln[\frac{N}{n_i}]\right\}^3 \left\{\frac{1}{x_g} - \frac{2}{3}\kappa(\frac{2\kappa\epsilon_o}{Nq}(\frac{kT}{q})ln[\frac{N}{n_i}])^{-1/2}\right\} \tag{3}$$

The open-gap J-II region constitutes a thermally-charged capacitor. As evident from (3), the device's capacitive energy varies strongly with temperature, scaling as $(T)^3$. This is not surprising since primary determinants of the energy are $V_{bi}$ and $x_{dr}$, both of which originate with thermal processes. Note, thermal capacitors can remain charged indefinitely since the open-gap configuration is an equilibrium state of the system [2].

Eq. (2) predicts the *standard device's* J-II region contains roughly three times the electrostatic potential energy of the J-I region ($\Delta\mathcal{E}_{es}(J-II) \sim 320$ eV). Equivalently, the whole device contains twice the energy in its open-gap configuration as it does in its closed-gap configuration, the majority of this excess energy in the J-II vacuum gap. When switched from open to closed, this excess energy is released. Thermodynamically, this may be viewed as simply the relaxation of the system from a higher energy (open-gap) to a lower energy (closed-gap) equilibrium state. (This Letter focuses on equilibrium states since the nonequilibrium physics (charging and discharging), though interesting, is too involved to consider here. Work extraction is also not considered except to note that schemes suitable for switching and electromechanical work extraction have been proposed or tested [3,4].)

Device output power $P_{dev}$ scales as: $P_{dev} \sim \frac{\Delta\mathcal{E}_{es}(J-II)}{\tau_{dis}}$, where $\tau_{dis}$ is the characteristic discharging time for the charged open-gap J-II region as it is closed. $\tau_{dis}$ can be short, on the order of $\tau_{dis} \simeq 10^{-6} - 10^{-8}$ sec, consistent with typical inverse slew rates of micron-sized p-n diodes; thus, the instantaneous power for a single, switched *standard device* is estimated: $P_{dev} \simeq 0.05 - 5 \times 10^{-9}$ W. Instantaneous power densities can be large; for the *standard device*, $\mathcal{P}_{dev} = \frac{P_{dev}}{(10^{-6}m)^3} \sim 0.05 - 5 \times 10^{9}$ $\mathrm{Wm}^{-3}$. Thermal capacitive energy and power densities compare well with those of their traditional microelectronic counterparts, suggesting they might play a role in future micro- and nanotechnology.

Positive energy release ($\Delta\mathcal{E}_{es} > 0$) is subject to limits in $x_g$, $N$, and $T$. From (2), an energy crossover ($+\Delta\mathcal{E}_{es}$) to ($-\Delta\mathcal{E}_{es}$) occurs at $x_g = \frac{3}{\kappa}x_{dr}$; for silicon, this is $x_g \simeq \frac{x_{dr}}{4}$. That is, only for $x_g \leq \frac{x_{dr}}{4}$ will net energy be released in switching from open- to closed-gap configurations. Since $x_{dr}$ is normally restricted to $x_{dr} \leq 10^{-5}$m, this implies $x_g \leq 2\times10^{-6}$m, thus, thermal capacitors must intrinsically be microscopic in the gap dimension; and, at least for the vacuum case, mechanical considerations will probably also similarly limit the other two dimensions. For this model, positive $\Delta\mathcal{E}_{es}$ are possible for moderately-doped semiconductors only; for nonconductors, charge diffusion is absent, thus, with no internal electric field, the capacitor does not charge; for good conductors (*e.g.*, metals or highly doped semiconductors), either $\kappa \gg 1$ or $x_{dr}$ is small, in which case Eqs. (2,3) predict $\Delta\mathcal{E}_{es} \leq 0$. Eq. (3) indicates that energy crossover for $N$ occurs for the *standard device* at $N \sim 10^{22}\mathrm{m}^{-3}$. Finally, $\Delta\mathcal{E}_{es} \longrightarrow 0$ when $T$ falls below the freeze-out temperature for charge carriers; for silicon, $T_{freeze} \leq 100$K.

Two-dimensional numerical simulations of the equilibrium states of the thermal capacitor were performed using Silvaco International's semiconductor Device Simulation Software [Atlas (S-Pisces, Giga)]. Output from the numerical

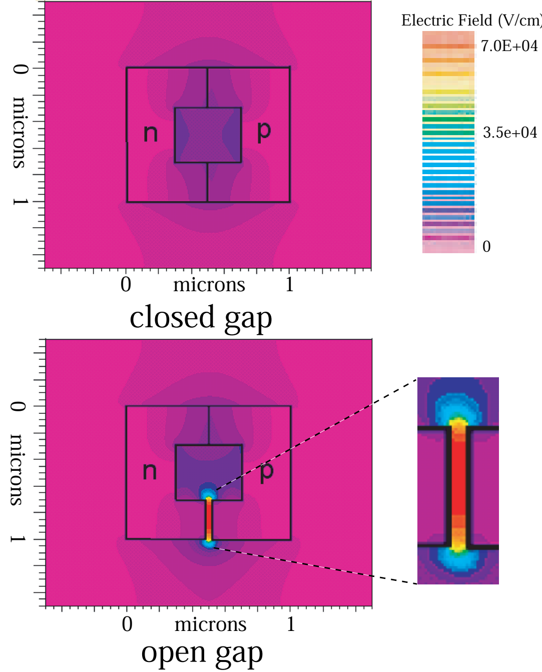


Figure 2: Atlas 2-D numerical simulations of electric field for closed-gap and open-gap configurations of the *standard device*. Sizes are given in $\mu$m, while field strength varies with color, scaling linearly from 0 V/cm (fuchsia) to $7 \times 10^4$ V/cm (red).

simulations were two-dimensional, simultaneous, equilibrium solutions to the Poisson, continuity, and force equations, using the Shockley-Read-Hall recombination model. Over a wide range of experimental parameters ($10^{17} \leq N_{A,D} \leq 10^{26}\text{m}^{-3}$; $10^{-8} \leq x_g \leq 3 \times 10^{-7}$m), the two-dimensional numerical simulations showed good agreement with the primary findings of the 1-D analytic model, most significantly that much larger electric fields can reside in the J-II vacuum gap than in the J-I junction, that significant electrostatic energy and electric charge are both stored in the J-II region and can be released upon switching, and that $\Delta\mathcal{E}_{es}$ crosses over as predicted. Differences between models can be traced primarily to the unrealistic discontinuities in physical parameters in the 1-D model, which are smoothed by the more realistic 2-D simulator.

Figure 2 displays the electric field magnitude for the open and closed gap configurations of the *standard device*. As expected, the electric fields for the closed state are modest ($|\mathbf{E}| \leq 10^6$ V/m) and are centered on the depletion regions, which, as predicted in the 1-D model, extend over the length of the device. While the electric fields in the J-I depletion regions of two cases are similar, in the J-II regions they are significantly different. The J-II electric

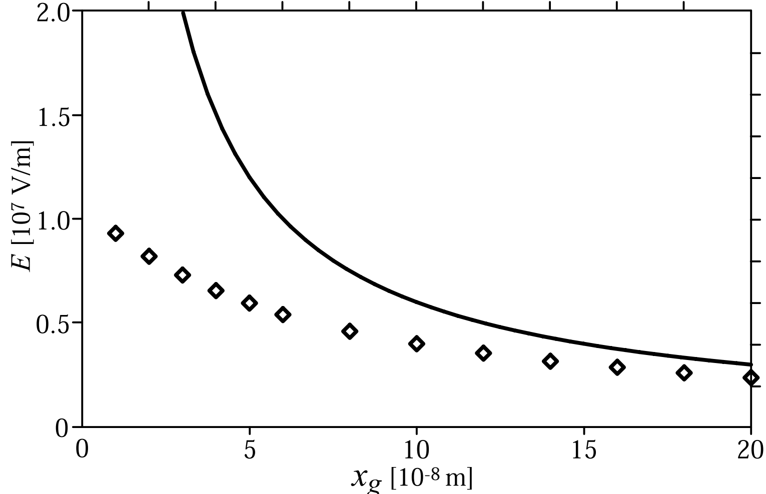


Figure 3: Electric field strength for *standard device* versus gap width $x_g$ calculated at the geometric center of the J-II region for 1-D analytic model (solid line) and 2-D numerical model (open diamonds).

field for the open state is $E \simeq 7 \times 10^6$ V/m (Fig. 2b) versus an average of $E \simeq 5 \times 10^5$ V/m (Fig 2a). Numerical integration of the electrostatic field energy over the entire region (vacuum and bulk) indicates the total electrostatic energy of the open-gap case is roughly 1.5 times that of the closed-gap case. Considering only the J-II region of each device, the open state stores roughly twice the electrostatic energy of the closed state. These are within 50% of the the energy estimates of the 1-D analytic model.

In Figure 3, the mid-channel electric field is plotted versus gap width for open-gap state of the *standard device*. Predictions of the 1-D analytic model (solid line) are compared with results of 2-D numerical simulations (open diamonds). The 1-D analytic model overestimates the electric field compared with the 2-D numerical simulation, particularly at small $x_g$, but this is expected given the 1-D model's unphysical singularity at $x_g = 0$. At small gap widths the 1-D model predicts the electric field should vary strictly as $\frac{1}{x_g}$, whereas in the 2-D model, the charge carriers in the bulk respond to the high fields, disperse, and thereby moderate them. As a result, the 2-D model consistently renders lower field strengths than the 1-D model, saturating at roughly $10^7$ V/m, safely below the dielectric strength of silicon. At larger gap widths the two models agree well.

Electrostatic potential energy is stored in the J-I and J-II regions of the thermal capacitor in both the open- and closed-gap configurations. In Figure 4, total device energy $\mathcal{E}_{es}$ is plotted versus $x_g$ for the *standard device*, comparing the 1-D and 2-D models. (Energy is normalized with respect to the $z$-direction (J/m) so as to conform with the output of the 2-D model.) The total electrostatic energy

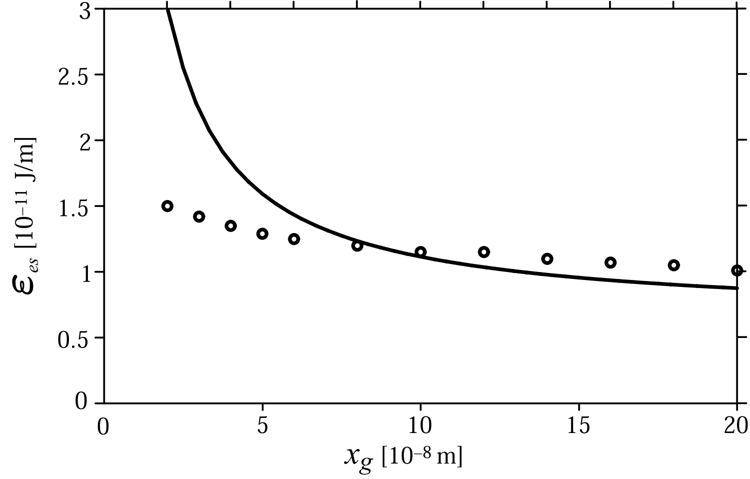


Figure 4: $Z$-normalized electrostatic potential energy $\mathcal{E}_{es}$ versus gap width ($x_g$) for standard device in 1-D model (solid line) and 2-D model (open circles).

is the sum of the contributions from the vacuum energy density ($\frac{\epsilon_o E^2}{2}$) and n-p bulk energy density ($\frac{\kappa\epsilon_o E^2}{2}$), integrated over their respective regions. For both models, the device energy decreases monotonically with increasing gap width, however their magnitudes and slopes differ due to the differing model assumptions. At small gap widths ($x_g \leq 10^{-7}$m), the 1-D model predicts greater energy than the 2-D model, owing principally to its vacuum energy, whereas at larger gap widths ($x_g \geq 10^{-7}$m) the energy in the 2-D model's n-p bulk dominates. (The 1-D model explicitly ignores energy contributions from the p-n bulk on either side of the vacuum gap.) In the density vicinity of the *standard device* the two models agree to within about 50%.

## References

1. G.W. Neudeck, *Vol. II: The pn junction diode* $2^{nd}$ edition, in *Modular series on solid state devices*, R.F. Pierret and G.W. Neudeck, editors. (Addison-Wesley, Reading, 1989).
2. Thermo-statistical fluctuations in charge and energy can be shown to be negligible.
3. N.C. MacDonald, in *Nanotechnology*, G. Timp, editor, (AIP-Springer-Verlag, New York, 1999). Chapter 3.
4. J.H. Wright, D.P. Sheehan, and A.R. Putnam, *Modeling a sub-micrometer electrostatic motor*, J. Nanosci. Nanotech., 3, 329-334, (2003).

-

-

**Acknowledgements:** This work was supported by a USD Faculty Research grant and DOE grant ER54544 and a Cottrell College grant from the Research Corporation.